Dissociation of DNA from Histone by Reaction of Anti-cancer Drug *cis*-Diamminedichloroplatinum(II) with DNA–Histone Complexes Used as Cellular Model

Yuhki KOYAMA, Sachie KIKUCHI, Sayaka NAKAGAWA, and Shigeki KOBAYASHI*

Division of Analytical Chemistry of Medicines, Showa Pharmaceutical University; 3–3165 Higashi-tamagawagakuen, Machida, Tokyo 194–8543, Japan. Received June 6, 2006; accepted January 12, 2007

Although both *cis*-diamminedichloroplatinum(II) (cisplatin or *cis*-DDP) and *trans*-diamminedichloroplatinum(II) bind to DNA, only *cis*-DDP is widely used as a chemotherapeutic agent; the stereoisomer *trans*-DDP is inactive. DNA, generally, is wound around the histone core in the nucleus of living cells and forms the nucleosome structure. To understand the essentially different anticancer activities of *cis*-DDP and *trans*-DDP, it is necessary to investigate the interaction of *cis*-DDP (or *trans*-DDP) with DNA around the histone in the nucleosome. Here, we used ϕX174DNA–histone^{LNCaP} complexes prepared by the reaction of ϕX174DNA with histone^{LNCaP} extracted from LNCaP cells. We first show that the ability of *cis*-DDP to dissociate the DNA from ϕX174DNA–histone^{LNCaP}, as a nucleosome model, is much stronger than that of *trans*-DDP. As a result of the action of *cis*-DDP, the DNA in the nucleosome is rendered naked, and the naked DNA is vulnerable to *cis*-DDP (or other drugs). This study describes a new model showing that the difference in the activities of *cis*-DDP and *trans*-DDP is related to the difference in their abilities to dissociate the DNA from the nucleosome.

Key words cisplatin; anticancer drug; DNA–histone complex model; cisplatin modified DNA–histone complex; electron microscopy

cis-Diamminedichloroplatinum(II), $Pt^{II}(NH_3)_2Cl_2$ (cisplatin or *cis*-DDP) is a useful anti-neoplastic agent in cancer chemotherapy. Many studies on the mechanism of this anticancer effect confirm that the bifunctional coordinate bonds between *cis*-DDP and cellular DNA are related to cell death.[1,2] However, the *trans*-isomer of *cis*-DDP is clinically ineffective although it binds to DNA. It is not yet clear why only *cis*-DDP is an antitumor drug.[3,4] One reason for this is that there is little information on tertiary structures of *cis*-DDP-modified DNA–histone complexes produced by the reaction of *cis*-DDP with a nucleosome. When *cis*- or *trans*-DDP binds to a DNA–histone complex, it seems that the higher-order structure of the DNA undergoes marked changes. The structure of *trans*-DDP-modified DNA–histone complexes may differ from that of *cis*-DDP-modified DNA–histone complexes. In our previous paper, we reported that *cis*-DDP is formed by change from negative (−) to positive (+) writhing number (Wr) binding to circular closed DNA.[5] Moreover, we found that topologically invariant trefoil and catenane are produced by the reaction of *cis*-DDP-modified DNA with DNA topoisomerase I.[6] Although the results suggest that similar products result from the binding of *cis*-DDP (or *trans*-DDP) with the DNA in cells, our previous model did not include histone–DNA complexes in the reaction model of *cis*-DDP with DNA.

The non-histone proteins HMG1 and HMG2 belong to the HMG1-box protein family, which is known to bind to distorted DNA structures and to bend and unwind DNA upon binding.[7,8] In addition, it has recently been reported that the linker histone H1 also binds to *cis*-DDP-modified DNA and that the binding affinity of linker histone H1 is greater than those of HMG1 and HMG2.[9] To increase understanding of the differences in the conformational changes that occur on modification of DNA by *cis*-DDP and *trans*-DDP, the preparation of histone–DNA complexes and *cis*-DDP-modified histone–DNA adducts is necessary. Here, we prepared *cis*-DDP-modified histone–DNA adducts using total core histones extracted from LNCaP cells. Our aim was to understand the topological difference between the structures of *cis*-DDP- and *trans*-DDP-modified histone–DNA complexes which are shown in Fig. 1.

In this study, we show (i) the fiber-like structure model of the histone–DNA complexes prepared by the incubation of ϕX174DNA with extracted core histones; and (ii) the change in DNA conformation that occurs on the binding of *cis*-DDP (and *trans*-DDP) with fiber-like DNA–histone complexes. The data on DNA length and topology obtained by electron microscopic analysis show that the action of *cis*-DDP is to dissociate DNA from histone in DNA–histone complexes. However, *trans*-DDP had a smaller dissociating effect than *cis*-DDP. We think that the dissociation of DNA from DNA–histone complexes provides important information on the different chemical and chemotherapeutical functions of *cis*-DDP and *trans*-DDP. To help us increase our understanding of the action of *cis*-DDP in the nucleus, we used *cis*-DDP- and *trans*-DDP-modified DNA–histone complexes as a *cis*-DDP- and *trans*-DDP-modified nucleosome model.

Experimental

Materials The platinum complexes, *cis*- and *trans*-$Pt(NH_3)_2Cl_2$, were purchased from Sigma-Aldrich Japan Inc. (Tokyo). Closed circular supercoiled SV40 DNA and ϕX174RF I DNA were from Gibco BRL (Rockville, MD, U.S.A.) and Takara Bio Inc. (Otu, Japan), respectively. Ethidium bromide and histone were from Sigma-Aldrich Japan Inc. and other chemicals were from Wako Pure Chemical Industries, Ltd. (Osaka, Japan).

Cell Lines and Cell Culture Human breast cancer MCF-7 and LNCaP[10] cells were obtained from Health Science Research Resources

Fig. 1. Structures of Cisplatin (**1**) and Transplatin (**2**)

* To whom correspondence should be addressed. e-mail: kobayasi@ac.shoyaku.ac.jp

Bank of Japan (Osaka, Japan) and Jikei University School of Medicine (Tokyo), respectively, and grown in phenol red-free RPMI1640 medium (Sigma, U.S.A.) containing 23.8 mM $NaHCO_3$ and supplemented with penicillin G (10000 units/l), streptomycin sulfonate (10 mg/l), and 10% fetal calf serum (FCS) (JRH Biosciences, U.S.A.) and 10% fetal bovine serum (FBS) (Sigma, U.S.A.). The cells were maintained in 75 cm^2 culture flasks and incubated at 37 °C in a humidified mixture of 5% CO_2 under atmospheric pressure. When the cell lines were used experimentally, they were first treated with trypsin–ethylenediaminetetraacetic acid (EDTA) (Cosmobio Co. Ltd, Japan) and then washed and resuspended in complete medium.

Histone Extraction from MCF-7 and LNCaP Cells Cultures allowed the cells in the confluent growth phase in a 75 $cm^2 \times 8$ culture flasks. The medium was replaced with (or without) 14 ml of medium, and each flask was incubated for 24 h. MCF-7 and LNCaP cells (about 3.2×10^8 cells/total) were harvested and collected by centrifugation (5 min at 1000 rpm) and the pellets were washed twice with cooled PBS(−). Histone extracts were obtained according to the method of Cousens *et al.*,[11] with minor modifications. The resulting precipitate was collected by centrifugation and dried in a vacuum for 5 min, then dissolved in 500 μl of 10 mM Tris–HCl (TH, pH 7.5) buffer and stored at −20 °C. We refer to the histones extracted from LNCaP and MCF-7 cells as histone^{LNCaP} and histone^{MCF7}, respectively, and to commercial histone (purchased from Sigama) as histone^{com}.

Quantitative Analysis of Histone The concentration of histone proteins extracted from LNCaP and MCF-7 cells was determined using the modified Lowry method (Bio-Rad, U.S.A.).

Preparation of DNA–Histone Complexes The ϕX174DNA–histone complexes were prepared by incubation of 10 mM TH buffer (pH 7.5) and 6 μl of a solution containing ϕX174DNA (0.096 μg) with 2 μl of a solution containing 0.556, 1.13, 2.01, 4.53, 9.05, 18.1, or 36.2 ng of histone^{LNCaP} at 37 °C for 40 min. SV40 DNA–histone^{LNCaP} complexes were prepared by a method similar to that described above. The ϕX174DNA–histone^{MCF7} complexes were prepared by incubation with 0.92, 1.84, 3.68, 7.35, 14.7, 29.4, or 58.8 ng of histone^{MCF7}. The mixtures were incubated for 60 min at 37 °C and terminated at −20 °C. The samples were analyzed by 0.8% agarose gel electrophoresis.

To confirm the results with SV40DNA and histones, we used the same method as that described above. SV40DNA–histone^{MCF7} complexes were prepared by incubation of 10 mM TH buffer (pH 7.5) and 6 μl of a solution containing SV40DNA (0.074 μg) with 2 μl of a solution containing 0.115, 0.231, 0.461, 0.923, 1.845, 3.69, or 7.38 ng of histone^{LNCaP} at 37 °C for 60 min. Similarly, SV40DNA–histone^{com} complexes were prepared by incubation of 10 mM TH buffer (pH 7.5) and 6 μl of SV40DNA (0.074 μg) with 2 μl of histone^{com} solution containing 9.2, 18.4, 36.8, 73.5, 147, 294, and 588 ng of histone^{com} at 37 °C for 30 min. The reactions were terminated at −20 °C. The samples were analyzed by gel electrophoresis with 0.8% agarose.

Preparation of *cis*-DDP- (or *trans*-DDP)-Modified DNA–Histone Complexes A stock solution of *cis*-DDP (2.5×10^{-2} M) was prepared by dissolving the complex in 10 mM TH buffer (pH 7.5). The *cis*-DDP-modified ϕX174DNA–histone^{LNCaP} complexes were prepared by the incubation of 6 μl of a solution containing 0.074 μg of ϕX174DNA–histone^{LNCaP} complexes for 0, 0.25, 0.5, 1.0, 3.0, 6.0, 8.0, 12.0, 24.0, 30.0, 48.0, or 72.0 h at a final concentration of 4.0×10^{-5} M of fresh *cis*-DDP with a solution (final volume 8 μl) containing 10 mM TH buffer at 37 °C and were stored at −20 °C in the dark. The reactions were terminated at −20 °C and analyzed by 0.8% agarose gel electrophoresis and electron microscopy.

Using a similar method, ϕX174DNA–histone^{LNCaP} complexes were incubated with 2 μl of *trans*-DDP for 0, 0.25, 0.5, 1.0, 3.0, 6.0, 8.0, 12.0, 24.0, 30.0, 48.0, and 72.0 h at a final concentration of 4.0×10^{-5} M of fresh *trans*-DDP.

Electrophoresis The complexes were loaded on an 0.8% agarose gel for electrophoresis in TBE (0.09 M Tris–borate, 0.002 M EDTA, pH 8.1) buffer at 15 V (1.5 V/cm) constant power for 16 h. The gels were stained with ethidium bromide (0.5 μg/ml) for 1 h in TBE buffer, and photographed under UV light with a Polaroid camera using Polapan 667 films.

Electron Microscopy The treatment of samples used for electron microscopy was essentially the same as that described by Yamagishi.[12] The grids were inserted into a JEOL JEM-SCAN100CX II electron microscope, so that the shadowed surface, subjected to rotary shadowcasting with tungsten (W), of the grid faced toward the emulsion side of the sheet film. Electron micrographs were taken at an initial magnification of 20000×. The counter lengths of platinum-modified DNA–histone complexes were determined by tracing from negatives of the enlarged image and measured with a MicroAnalyzer version 1.1d (Nihon Poladigital, Ltd., Tokyo).

Results

Preparation of DNA–Histone Complexes with ϕX174DNA and SV40 DNA To establish a simple means of preparing DNA–histone complexes, we investigated a method of incubating ϕX174DNA (or SV40DNA) with histone^{MCF7} (or histone^{LNCaP}) in 10 mM Tris–HCl buffer (pH 7.5). The ϕX174DNA– and SV40DNA–histone complexes were detected using 0.8% agarose gel electrophoresis, and the changes in electrophoretic mobilities as a function of the amount of histones are shown in Fig. 2.

Figure 2A shows that the gel mobility of the bands decreased with increasing amount of histone^{LNCaP}; the amounts of histone^{LNCaP} are shown in the upper part of the gels. A similar trend was also observed for the incubation of ϕX174DNA (0.074 μg/tube) with histone^{MCF7} (Fig. 2B). The gel mobility of ϕX174DNA–histones^{MCF7} complexes decreased strikingly as the amount of histone^{MCF7} increased. This suggests aggregation of the ϕX174DNA–histone complexes. Therefore, electrophoretic mobility decreases toward the top of the gel (Figs. 2A, B, lanes 2—4 and lanes 2—6, respectively). However, the DNA–histone complexes indicated by the arrows are soluble complexes and the bands are shifted to the middle of the gels. The complexes are not aggregated like those at the top of the gel.

To confirm the formation of DNA–histone complexes, SV40DNA and SV40DNA–histone^{com} complexes were used as a comparison with ϕX174DNA–histones^{LNCaP} and ϕX174DNA–histones^{MCF7} complexes. SV40DNA was modified with the histone^{com} and the SV40DNA–histone^{com} complexes thus obtained were analyzed by 0.8% agarose gel electrophoresis (Fig. 3A). Figure 3B shows the changes in the electrophoretic mobility of the SV40DNA–histone^{MCF7} complexes prepared by the incubation of SV40DNA with histone^{MCF7}. The striking decreases in the gel mobility of the SV40DNA–histone^{MCF7} and SV40DNA–histone^{com} complexes on addition of increasing amounts of histone are similar to those found with the ϕX174DNA–histone^{LNCaP} and ϕX174DNA–histone^{MCF7} complexes.

Structure and Length of DNA–Histone Complexes We analyzed the length, size, and shape of the DNA–histone complexes using an electron microscope. Electron mi-

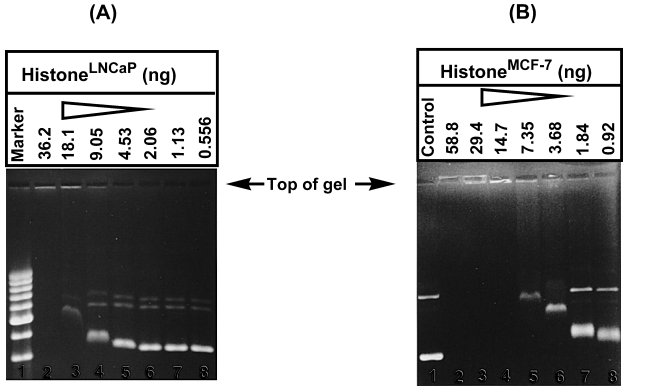

Fig. 2. Agarose Gel Electrophoresis of ϕX174RF DNA–Histone Complexes Produced by Reaction of ϕX174RF DNA with Histone Extracted from Cells

(A) Lane 1 shows a 1 kb DNA ladder marker. Lanes 2—7 contain histone of 36.2, 18.1, 9.05, 4.53, 2.06, 1.13, and 0.56 ng, respectively. Mixtures of ϕX174RF DNA (0.074 μg) and histones^{LNCaP} were incubated for 40 min at 37 °C. (B) Lane 1 contains ϕX174RF DNA (0.074 μg). Lanes 2—7 contain histones^{MCF7} of 58.8, 29.4, 14.7, 7.35, 3.68, 1.84, and 0.92 ng, respectively.

croscopy visualization was performed by magnifying membranes fixed on solutions of DNA–histone complexes treated with formamide buffer (20 mM TH, 2 mM EDTA, 50 v/v% formamide) solution at 20000× or 28000×. As the samples used for electron microscopy were treated with formamide buffer, the tertiary structure and interaction of the DNA–histone complexes would be expected to be destroyed because formamide is a denaturation reagent. However, the results of electron microscopy visualization indicated that the binding between the DNA and histone was strong. Figure 4 shows electron micrographs of the SV40DNA–histone^{com} (Fig. 4B) and ϕX174DNA–histone^{LNCaP} complexes (C) at different concentrations of the histones. The electron micrographs shown in Fig. 4A**ia** and **ib** correspond to SV40DNA only in lane 8 in Fig. 3A and ϕX174DNA only in lane 1 in Fig. 2B, respectively. The electron micrograph shown in Fig. 4B**iia** corresponds to the sample tube of the gel in lane 5 (in Fig. 3A) and the electron micrograph in Fig. 4B**iib** is an enlargement of that shown in Fig. 4B**iia**. The electron micrographs shown in Fig. 4C**iiia** (and **iiib**) and **iva** (and **ivb**) correspond to the sample tubes of lanes 4 and 7 in Fig. 2A, respectively. From these electron micrographs, it is clear that the structures of the ϕX174DNA–histone^{LNCaP} and SV40DNA–histone^{com} complexes are of folding, branched, and fiber-like shape. The fiber-like shape is very similar to the conformation published previously.[13] These results indicate that the resulting complexes provide a simple model of the chromatin-like structure or a nucleosome-like structure such as that of the chromatin or nucleosome in the nucleus of the living cell. Although the controls of ϕX174DNA and SV40DNA are typically superherical and relaxed structures, as shown in Fig. 4A, the ϕX174DNA–histone^{LNCaP} complexes show a branched conformation (Fig. 4C). Clearly, the shape of the complexes is different to that of ϕX174DNA.

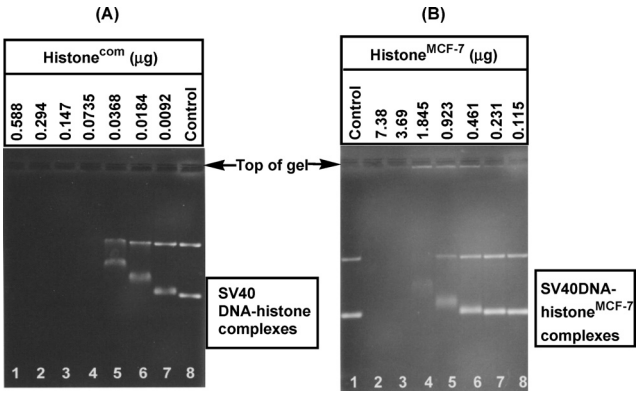

Fig. 3. Agarose Gel Electrophoresis of SV40DNA–Histone Complexes Produced by Reaction of SV40DNA with Histones Extracted from Cells

(A) Lanes 1—8 contain SV40DNA (0.063 μg). Lanes 1—7 contain histones of 588, 294, 147, 73.5, 36.8, 18.4, and 9.2 ng, respectively. Mixtures of SV40DNA (0.063 μg) and histones^{com} were incubated for 30 min at 37 °C and terminated at −20 °C. (B) Lane 1 contains SV40DNA (0.074 μg). Lanes 2—8 contain histone^{MCF7} of 7.38, 3.69, 1.845, 0.923, 0.461, 0.231, and 0.115 μg, respectively. Histone^{MCF7} was extracted from MCF-7 cells.

To estimate the length of the ϕX174DNA–histone^{LNCaP} complexes statistically, we measured the length of the DNA. Figure 5 shows the length distribution of the DNA in the samples corresponding to the gel lanes 4 and 7 in Figs. 2A and B, respectively. By tracing from the negatives of the enlarged image (×5), the lengths of the DNA and DNA–histone complexes were measured with a MicroAnalyzer. The mean length of ϕX174DNA was 1.70 μm and the amount (n) of DNA observed was 166. It is clearly seen that the length of ϕX174DNA decreases with increasing amount of histone^{LNCaP}. In the gel lane 4 in Fig. 2A, the mean length of the ϕX174DNA–histone^{LNCaP} complexes (n=374 molecules) is 1.59 μm. The diagram has two peaks (mean=0.95 and 1.45 μm, respectively) and the modal value is 1.45 μm. The histgrams in Figs. 5A and B do not follow the normal distribution. The visualized ϕX174DNA–histone^{LNCaP} complexes are compactly folded, as shown in the electron micrographs in Figs. 5A and B.

The results of the shape distribution of the fiber-like structures and the other topoisomers are listed in Table 1. Here, the shapes of the topoisomers **3**, **4**, scc, and relaxed are equal

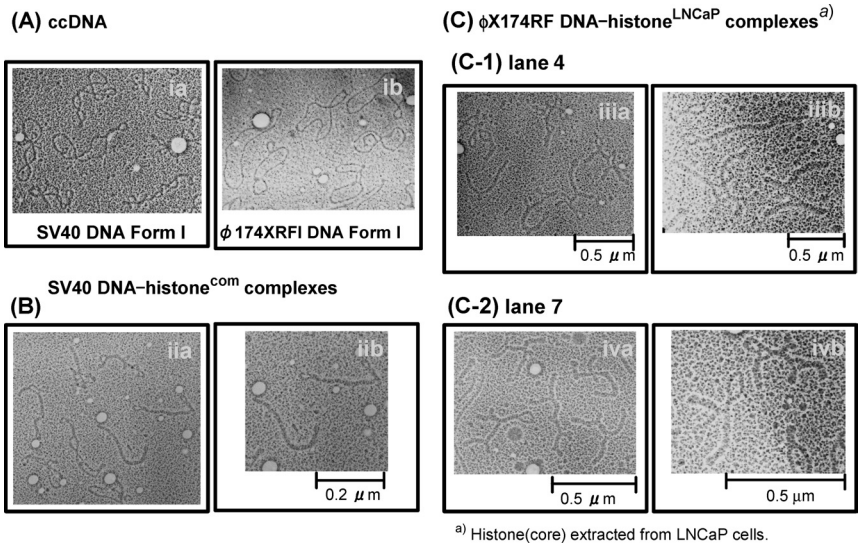

Fig. 4. Electron Micrographs of SV40DNA–Histone and ϕX174DNA–Histone Complexes as a Model of Nucleosomes

(A) Electron micrographs of SV40DNA (**ia**) and ϕX174DNA (**ib**) used in these studies. (B) Electron micrographs of SV40DNA–histone^{MCF7} complexes shown in lane 5 (**iia** and **iib**) in Fig. 3A. (C) Electron micrographs of ϕX174DNA–histone^{LNCaP} complexes shown in lane 4 (**iiia** and **iiib**) and lane 7 (**iva** and **ivb**) in Fig. 2A. Magnification 28000× or 20000×. The bar represents the scale (μm).

Table 1. Shape Distribution of Fiber-Like Complexes Prepared by Reaction of Closed Circular DNA with Histone Extracted from Culture Cells

Type	Shape distribution (%)					Total (%) (Amount)[f]
	Fiber-like[a] structure	Topo-isomer[b] (**3**)	Topo-isomer[c] (**4**)	Super-coils[d]	Relax[e] form	
SV40–Histone[MCF7 g]	70.5	7.6	7.4	10.6	3.9	100.0 (488)
ϕX174–Histone[LNCaP h]	62.5	9.4	—	22.2	5.3	99.4 (941)
ϕX174–Histone[LNCaP i]	51.8	12.3	7.8	17.7	7.2	96.8 (514)

a) See Fig. 5. *b*) DNA with one knot. *c*) DNA with two knots. *d*) DNA with three more knots. *e*) DNA without knot. *f*) Number of DNA observed by electron microscope. *g*) Histone[MCF7] extracted from MCF-7 cells. *h*) Histone[LNCaP] extracted from LNCaP cells. Lane 7 in Fig. 2A. *i*) Lane 4 in Fig. 2A.

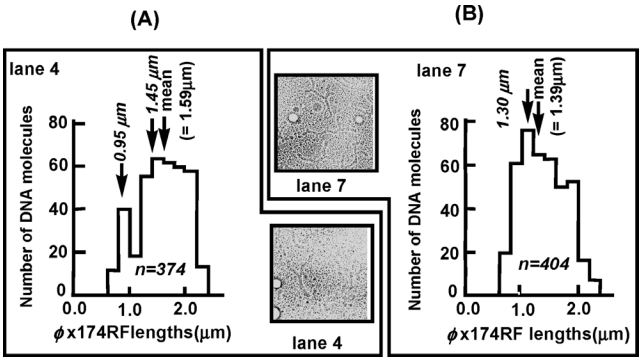

Fig. 5. Length Distribution of ϕX174DNA–Histone[LNCaP] Complexes

(A) Length distribution of ϕX174DNA–histone[LNCaP] complexes shown in lane 4 in Fig. 2A. Mean length is 1.59 μm (n=374 DNA molecules). Two peaks occur in the length distribution: the molecule lengths at the peaks are 0.95 and 1.45 μm, respectively. (B) Length distribution of ϕX174DNA–histone[LNCaP] complexes shown in lane 7 in Fig. 2A. Mean length is 1.39 μm (n=404 DNA molecules). The length distribution shows one peak: the molecule length at the peak is 1.30 μm. The mean length of ϕX174DNA used in this study is 1.70 μm (n=166 DNA molecules). All data shown in the histograms were obtained by electron microscopy.

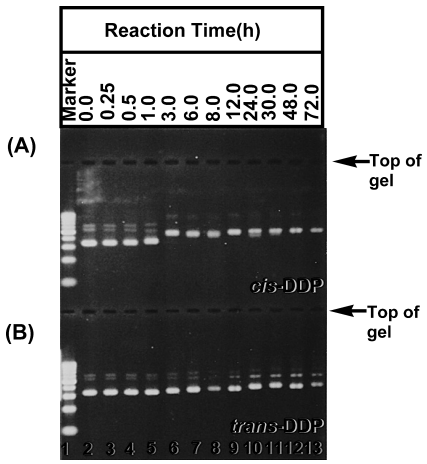

Fig. 6. Changes in Electrophoretic Mobility of (A) *cis*-DDP and (B) *trans*-DDP Modified ϕX174DNA–Histone Complexes

(A and B) Lane 1 is a 1 kb DNA ladder marker. Lanes 2—13 each contain ϕX174DNA–histone complexes prepared by reaction of ϕX174 DNA (0.074 μg) with histone[LNCaP] prepared under the same conditions as those in Fig. 2A. The complexes were incubated in the presence of fresh *cis*-DDP (final concentration of 4.0×10^{-5} M) (or *trans*-DDP) at 37 °C for 0, 0.25, 0.5, 1.0, 3.0, 6.0, 8.0, 12.0, 23.0, 30.0, 48.0, or 72.0 h.

to the topological shapes, □○□, □○□, superherical circular closed (=scc), and □, respectively. The knot number is one (=**3**), two (=**4**), N (=scc), and zero (=relax), respectively. The distribution (%) was calculated as the ratio of (m [measured amount of corresponding topoisomer]/n [total DNA amount])×100. Comparison of the results listed in Table 1 shows that the distribution ratio of the fiber-like structures is about 52—71% and we think that the winding of the histone[LNCaP] on the ϕX174DNA is the major reaction under our experimental condition.

Preparation of *cis*-DDP- (or *trans*-DDP)-Modified DNA–Histone Complexes To understand the difference in the binding style of *cis*-DDP and *trans*-DDP to DNA–histone complexes, *cis*-DDP- (or *trans*-DDP)-modified ϕX174DNA–histone[LNCaP] complexes were prepared by incubation of fresh *cis*-DDP and *trans*-DDP (at final concentration of 4.0×10^{-5} M) with ϕX174DNA–histone[LNCaP] complexes (prepared under the same reaction condition as that used in lane 4 in Fig. 2A) in 10 mM TH buffer. The reactions were time-dependent and were stopped by reducing the temperature to −20 °C. Figure 6 shows the results of 0.8% agarose gel electrophoretic analysis. In lane 6 in Fig. 6A, a marked change in the mobility of *cis*-DDP-modified ϕX174DNA–histone[LNCaP] complexes can be seen after an incubation time of 3 h. The mobility of the gel band is discontinuous between 1 and 3 h. However, the mobility after a reaction of 3 h is almost flat against the top of the gel. On the other hand, such a drastic change was not observed in the reaction of *trans*-DDP (final concentration 4.0×10^{-5} M) with ϕX174DNA–histone[LNCaP] complexes (lane 6 in Fig. 6B). The electrophoretic mobility of the *trans*-DDP-modified ϕX174DNA–histone[LNCaP] complexes is almost constant, as observed in lanes 2—13.

The results are obviously different from those by incubation of Pt^{2+} (*cis*-DDP and *trans*-DDP) with DNA without histone demonstrated in our previous paper.[5] The electrophoretic mobility of ϕX174DNA–histone[LNCaP] complexes is discontinuous in time-dependent or concentration-dependent reactions with *cis*-DDP. The changes in gel mobility may be related to conformation changes occurring during interactions between *cis*-DDP and DNA–histone complexes. To confirm the cause of the discontinuous shift in the gel band, we analyzed the structure using electron microscopy.

Length and Structure of *cis*-DDP- (or *trans*-DDP)-Modified DNA–Histone Complexes Figure 7 shows electron micrographs of the *cis*-DDP- (or *trans*-DDP)-modified ϕX174DNA–histone[LNCaP] complexes produced by incubation of *cis*-DDP (or *trans*-DDP) with ϕX174DNA–histone[LNCaP] complexes. In reactions of *cis*-DDP with ϕX174DNA–histone[LNCaP] complexes for 0.25 h, the complex is visualized as fiber-like DNA, as shown in the micrograph **va** in Fig. 7A (under the same reaction condition as that for lane 3 in Fig. 6). However, after a reaction for 6 h with *cis*-DDP, we observed that the ϕX174DNA in ϕX174DNA–histone[LNCaP] complexes of fiber-like shape was dissociated from the his-

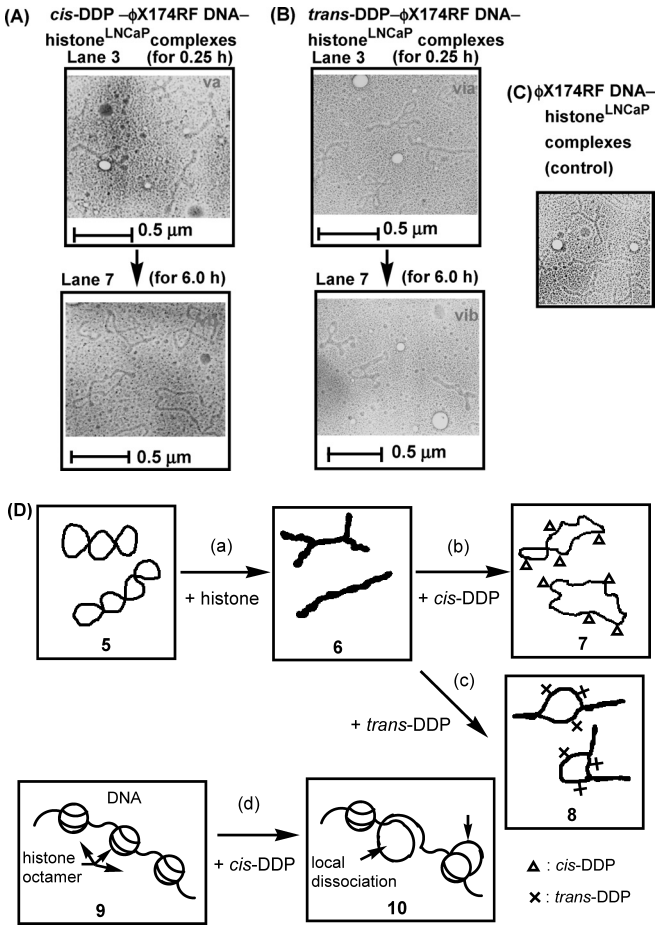

Fig. 7. Electron Micrographs of DNA Dissociated by Reaction of *cis*-DDP (or *trans*-DDP) with the Nucleosome Model (A, B, and C) and Illustration of Pathway of Dissociation of DNA

(A) Time course of the dissociation of ϕX174DNA from ϕX174DNA–histone^{LNCaP} complexes by treatment of fresh *cis*-DDP (final concentration of 4.0×10^{-5} M) for 0.25 h and 6.0 h, respectively: **va**, lane 3 (in Fig. 6A) and **vb**, lane 7 (in Fig. 6A). (B) Time course of the dissociation of ϕX174DNA from ϕX174DNA–histone^{LNCaP} complexes by treatment with fresh *trans*-DDP for 0.25 h and 6.0 h, respectively: **via**, lane 3 (in Fig. 6B); **vib**, lane 7 (in Fig. 6B). (C) ϕX174DNA–histone^{LNCaP} complexes (control). Magnification is 28000× or 20000×. The bar represents the scale (μm). (D) The negative closed superherical ϕX174DNA (**5**) used in this study is shown as an example. ϕX174DNA–histone^{LNCaP} complexes (**6**) had a fiber-like shape resulting from the reaction of histone^{LNCaP} with DNA **5** (path a). The dissociation of the DNA (**7**) occurred on addition to the complexes (**6**) of *cis*-DDP (path b). However, the dissociation of the DNA (**8**) on addition to the complexes (**6**) of *trans*-DDP was considerably less than that with *cis*-DDP (path c). A model of local dissociation (**10**) of DNA from the nucleosome (**9**) in living cells (path d). The bar represents the scale (μm).

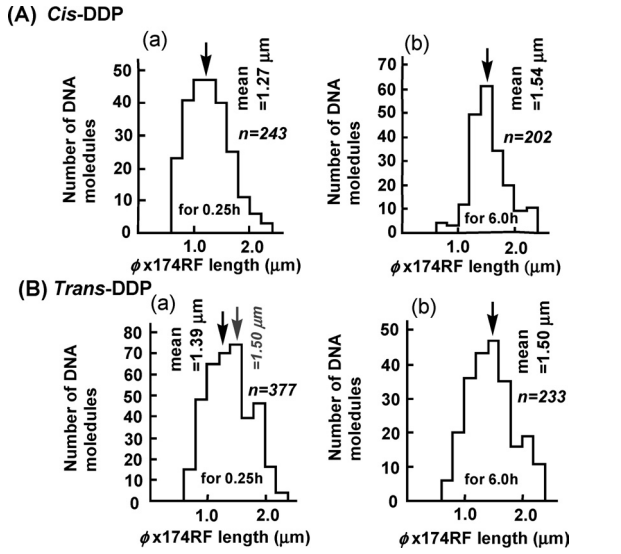

Fig. 8. Length Distribution of *cis*-DDP- and *trans*-DDP-Modified ϕX174DNA–Histone^{LNCaP} Complexes

(A) (a) Length distribution of the ϕX174DNA–histone^{LNCaP} complexes shown in lane 3 in Fig. 6A. Mean length is 1.27 μm (n=243 DNA molecules). (b) Length distribution of the ϕX174DNA–histone^{LNCaP} complexes shown in lane 7 in Fig. 6A. Mean length is 1.54 μm (n=202). (B) (a) Length distribution of the ϕX174DNA–histone^{LNCaP} complexes shown in lane 3 in Fig. 6B. Mean length is 1.50 μm (n=377). (b) Length distribution of the ϕX174DNA–histone^{LNCaP} complexes shown in lane 7 in Fig. 6B. Mean length is 1.50 μm (n=233). All data in the histograms were obtained by electron microscopy.

tone^{LNCaP} and unwound to the structure of the most relaxed-like DNA, as shown in micrograph **vb** in Fig. 7A (under the same reaction condition as that in lane 7 in Fig. 6A).

However, we found that ϕX174DNA almost dissociated from the histone^{LNCaP} complexes in the reaction of *trans*-DDP with ϕX174DNA–histone^{LNCaP} complexes for 0.25 h, as shown in the micrograph **via** in Fig. 7B (under the same reaction condition as that in lane 3 in Fig. 6B). In the reaction of *trans*-DDP with ϕX174DNA–histone^{LNCaP} complexes for 6.0 h (under the same reaction condition as that in lane 7 in Fig. 6B), the dissociation of ϕX174DNA from the histone^{LNCaP} was much less than that of *cis*-DDP, as shown in micrograph **vib** in Fig. 7B. Micrograph **vii** shows ϕX174DNA–histone^{LNCaP} complexes as a control. The shapes of ϕX174DNA in micrographs **via** and **vib** are similar to those of the control ϕX174DNA–histone^{LNCaP} complexes (**vii**).

The lengths of ϕX174DNA in *cis*-DDP and *trans*-DDP modified ϕX174DNA–histone^{LNCaP} complexes were measured using an electron microscope. The statistical result is summarized in Fig. 8. At time 0.25 h (lane 3) and 6.0 h (lane 7) in Fig. 6A, the mean length of the *cis*-DDP-modified DNA–histone complexes was 1.27 and 1.54 μm, respectively (Fig. 8A). The statistical difference is about 0.27 μm (1.54—1.27 μm). Therefore, it can be seen that ϕX174DNA molecule loosens and is long, and that the ϕX174DNA is dissociated from the ϕX174DNA–histone^{LNCaP} complexes.

In the reaction of *trans*-DDP with ϕX174DNA–histone^{LNCaP} complexes, however, the difference in mean length was 0.11 μm (1.50—1.39 μm) at times 0.25 h (lane 3) and 6.0 h (lane 7) (Fig. 8Ba, b). In Fig. 8Ba, the statistical length of the DNA shows almost no changes since the difference in the mode and mean values of DNA length was about 0 μm (1.50—1.50 μm). The results suggest that *trans*-DDP has little ability to dissociate ϕX174DNA from ϕX174DNA–histone^{LNCaP} complexes.

Discussion

Our aim in this study was to elucidate the conformational changes in DNA that occur on the binding of *cis*-DDP and *trans*-DDP to DNA–histone complexes. Although *cis*-DDP or *trans*-DDP is bound to DNA–histone complexes in the nucleus, the conformational changes of the DNA remain uncertain. It is believed that the changes that occur in DNA structure are strongly related to the anti-cancer activity of *cis*-DDP and *trans*-DDP. We describe here a new nucleus model using ϕX174DNA–histone complexes to improve our understanding of the roles of *cis*-DDP and *trans*-DDP in conformational changes in DNA. Many studies of the nucleus

model using DNA–histone complexes have been performed by mixing histone H1 with DNA (and synthetic fragment DNA, *etc.*).[13,14] In our study, the DNA–histone complexes were prepared by reaction of ϕX174DNA with histones extracted from LNCaP and MCF-7 cells. In our analysis of the shapes and structures of ϕX174DNA–histone^{LNCaP}, ϕX174DNA–histone^{MCF7}, and SV40DNA–histone^{MCF7} complexes, electron microscopy visualization demonstrated the production of compact fiber-like DNA–histone complexes. Agarose gel electrophoresis also clarified the formation of DNA–histone complexes by a shift in electrophoretic mobility. The statistical analysis indicated that the fiber-like complexes were obtained with a yield of about 52—70%. The shape of the fiber-like complexes is similar to that in the data of lit[13] produced by treatment of pBR322 DNA with histone H1. Thus, we have described a model of nucleosome-like complexes (Fig. 4C) obtained by incubation of ϕX174DNA with histone^{LNCaP} extracted from LNCaP cells. We think that the band at the top of the gel is formed by aggregation based on the interaction between DNA–histone complexes (lanes 2, 3 in Fig. 2). The band are insoluble. Thus, the production of DNA–histone complexes can be monitored as a gel shift.

To elucidate the change in DNA structure in the nucleus of cells, we performed an electrophoretic and electron microscopic study of *cis*-DDP- and *trans*-DDP-modified DNA by the reaction of *cis*-DDP and *trans*-DDP with DNA–histone complexes in a nucleosome model. Electron microscopic visualization showed that *cis*-DDP is able to dissociate the DNA from DNA–histone complexes. Evidently, ϕX174DNA easily dissociates from ϕX174DNA–histone^{LNCaP} complexes (Figs. 7A, B). Therefore, the large changes in gel mobility, which can be observed in lanes 5 and 6 in Fig. 6A may be related to the dissociation of ϕX174DNA from the complexes. However, such an inflection point is not observed on the gel electrophoresis shown in Fig. 6B. Lanes 5 and 6 in Fig. 6B suggest that *trans*-DDP modified ϕX174DNA–histone^{LNCaP} complexes are not dissociated to *trans*-DDP modified ϕX174DNA and histone^{LNCaP}. Electron microscope visualization supports the idea that the complexes do not contribute to the dissociation of *trans*-DDP modified ϕX174DNA and histone^{LNCaP}.

A similar result was observed in SV40DNA–histone^{MCF7} complexes prepared by incubation of histone^{MCF7} extracted from MCF-7 cells with SV40DNA. Although the dissociation of DNA from DNA–histone complexes (**6**) is accelerated by *cis*-DDP binding (path b in Fig. 7D), the geometrical isomer, *trans*-DDP, delays the dissociation of DNA from DNA–histone complexes, as shown in path c in Fig. 7D. The evidence suggests that DNA is locally dissociated from the nucleosome attacked by *cis*-DDP (path d in Fig. 7D). We think that DNA (**10**) locally dissociated from histone octamer may exist in the nucleus of living cells. Our results are relevant to the understanding of the difference in biological efficacy between *trans*-DDP and *cis*-DDP-modified DNA–histone complexes. Many studies have used *cis*-DDP- or *trans*-DDP-modified DNA as study material. However, we have pointed out the importance of DNA–histone complexes as the cellular target for *cis*-DDP.

Conclusion

We prepared ϕX174DNA–histone complexes by reaction of histone extracted from LNCaP and MCF-7 cells with ϕX174DNA and SV40DNA. These complexes may provide a simple model system for the nucleosome which has a fiber-like structure. Using DNA–histone complexes, we found that the binding interaction of *cis*-DDP, an anti-cancer drug, with DNA is able to dissociate the DNA from DNA–histone complexes more easily than *trans*-DDP. In living cells, the easy local disassociation of DNA from the nucleosome may be an important aspect of the anit-cancer activity of *cis*-DDP in both biophysical and chemotherapeutic processes. Finally, we think that it would be useful to increase our understanding of changes in DNA structure in the reactions of *cis*-DDP and *trans*-DDP with ϕX174DNA–histone complexes as a nucleosome model and to develop more active analogs of *cis*-DDP and other metals.

References

1) Rosenberg B., "Chemistry and Biochemistry of a Leading Anticancer Drug," ed. by Lippert B., Wiley-VCH, Zürich, 1999, pp. 3—30.
2) Montero E. I., Perez J. M., Schwartz A., Fuertes M. A., Malinge J. M., Alonso C., Leng M., Navarro-Ranninger C., *Chembiochem*, **3**, 61—67 (2002).
3) Zwelling L. A., Kohn K. W., *Cancer Treatment Reports*, **63**, 1439—1444 (1979).
4) Reedijk J., *Pure Appl. Chem.*, **59**, 181—192 (1987).
5) Kobayashi S., Nakamura N., Maehara T., Hamashima H., Sasatsu Y., Asano K., Ohishi Y., Tanaka A., *Chem. Pharm. Bull.*, **49**, 1053—1060 (2001).
6) Kobayashi S., Furukawa M., Dohi C., Hamashima H., Arai T., Asano K., Tanaka A., *Chem. Pharm. Bull.*, **47**, 1053—1060 (1999).
7) Pil P. M., Lippard S. J., *Science*, **256**, 234—237 (1992).
8) Ohndorf U. M., Rould M. A., He Q., Pabo C. O., Lippard S. J., *Nature* (London), **399**, 708—712 (1999).
9) Yaneva J., Leuba S. H., van Holde K., Zlatanova J., *Proc. Natl. Acad. Sci. U.S.A.*, **94**, 13448—13451 (1997).
10) Horoszewicz J. S., Leong S. S., Kawinski E., Karr J. P., Rosenthal H., Chu T. M., Mirand E. A., Murphy G. P., *Cancer Res.*, **43**, 1809—1818 (1983).
11) Cousens L. S., Gallwitz D., Alberts B. M., *J. Biol. Chem.*, **254**, 1716—1723 (1979).
12) Yamagishi H., "Chemistry of Nucleic Acid II," ed. by The Japanease Biochemical Society, Tokyo Kagaku Dojin, Tokyo, 1989, p. 389.
13) Sogo J., Stasiak A., DeBernardin W., Losa R., Koller T., "Electron Microscopy in Molecular Biology," ed. by Sommerville J., Scheer U., IRL Press, Oxford, 1987, pp. 61—79.
14) Buttinelli M., Leoni L., Sampaolese B., Savino M., *Nucleic Acids Res.*, **19**, 4543—4549 (1991).